

3



AD A104495

RANDOM ERROR PROPAGATION ANALYSIS IN THE PLUME DIAGNOSTIC CODE EMABIC

Stephen J. Young

The Aerospace Corporation
El Segundo, California 90245

July 1981

SEP 22 1981

A

Approved for Public Release; Distribution Unlimited

DMC FILE COPY

Prepared for

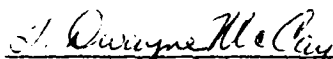
AIR FORCE ROCKET PROPULSION LABORATORY
DIRECTOR OF SCIENCE AND TECHNOLOGY
AIR FORCE SYSTEMS COMMAND
EDWARDS AFB, CALIFORNIA 93523

81 9 22 823
207500


FOREWORD


This report was submitted by the Aerospace Corporation, P.O. Box 92957, Los Angeles, California, 90009, under Procurement Directive AFRPL/SD 81-1, Job Order No. 573010CU with the Air Force Rocket Propulsion Laboratory, Edwards AFB, California 93523.

This report has been reviewed by the Technical Information Office (STINFO/TSPR) and is releasable to the National Technical Information Service (NTIS). At NTIS it will be available to the general public, including foreign nations. This technical report has been reviewed and is approved for publication; it is unclassified and suitable for general public release.


T. DWAYNE McCAY
Research Physical Scientist


GREGORY S. MESERVE, 1Lt, USAF
Project Manager


DAVID M. MANN
Chief, Plume Technology Branch


EUGENE G. HABERMAN
Chief, Propulsion Analysis Division

A

NOTICE

When U.S. Government drawings, specifications, or other data are used for any purpose other than a definitely related government procurement operation, the government thereby incurs no responsibility nor any obligation whatsoever, and the fact that the government may have formulated, furnished, or in any way supplied the said drawings, specifications, or other data, is not to be regarded by implication or otherwise, or in any manner licensing the holder or any other person or corporation, or conveying any rights or permission to manufacture or use, or sell any patented invention that may in any way be related thereto.

UNCLASSIFIED

SECURITY CLASSIFICATION OF THIS PAGE (When Data Entered)

REPORT DOCUMENTATION PAGE		READ INSTRUCTIONS BEFORE COMPLETING FORM
1. REPORT NUMBER AFRPL-TR-81-59	2. GOVT ACCESSION NO. AD-A104 495	3. RECIPIENT'S CATALOG NUMBER
4. TITLE (and Subtitle) RANDOM ERROR PROPAGATION ANALYSIS IN THE PLUME DIAGNOSTIC CODE EMABIC		5. TYPE OF REPORT & PERIOD COVERED
7. AUTHOR(s) Stephen J. Young		6. PERFORMING ORG. REPORT NUMBER TR-0081(6623)-2
9. PERFORMING ORGANIZATION NAME AND ADDRESS The Aerospace Corporation El Segundo, Calif. 90245		8. CONTRACT OR GRANT NUMBER(s) F04701-80-C-0081
11. CONTROLLING OFFICE NAME AND ADDRESS Air Force Rocket Propulsion Laboratory Edwards Air Force Base, Calif.		10. PROGRAM ELEMENT, PROJECT, TASK AREA & WORK UNIT NUMBERS
14. MONITORING AGENCY NAME & ADDRESS (if different from Controlling Office)		12. REPORT DATE July 1981
		13. NUMBER OF PAGES 30
		15. SECURITY CLASS. (of this report) Unclassified
		15a. DECLASSIFICATION/DOWNGRADING SCHEDULE
16. DISTRIBUTION STATEMENT (of this Report) Public Release; Distribution Unlimited		
17. DISTRIBUTION STATEMENT (of the abstract entered in Block 20, if different from Report)		
18. SUPPLEMENTARY NOTES		
19. KEY WORDS (Continue on reverse side if necessary and identify by block number) Inversion Methods Error Propagation Rocket Plume Radiation		
20. ABSTRACT (Continue on reverse side if necessary and identify by block number) The formal theory of linear error propagation is applied to the data smoothing and profile inversion routines of the plume diagnostic code EMABIC. In addition to the normal operation of retrieving the radial temperature and concentration profiles of the plume from measured transverse profiles of emission and absorption, EMABIC can now automatically estimate the accuracy of retrieval from estimates of the experimental random error of the measurements. An application of the method is made for a case previously examined with an empirical error propagation method. The present results are essentially in		

DD FORM 1473
(IF ASSIMILE)

UNCLASSIFIED

SECURITY CLASSIFICATION OF THIS PAGE (When Data Entered)

UNCLASSIFIED

SECURITY CLASSIFICATION OF THIS PAGE(When Data Entered)

19. KEY WORDS (Continued)

20. ABSTRACT (Continued)

agreement with those of the previous study.

UNCLASSIFIED

SECURITY CLASSIFICATION OF THIS PAGE(When Data Entered)

CONTENTS

1.	INTRODUCTION	5
2.	ERROR PROPAGATION THEORY	7
2.1	General Theory	7
2.2	Error Propagation through Presmoothing	10
2.3	Error Propagation through Inversion	15
3.	EXAMPLE APPLICATION	20
	APPENDIX -- Error Propagation Control Cards for EMABIC	27

FIGURES

1.	Transtage Temperature and Gas Concentration Profiles	21
2.	Transtage Pressure Profile	22
3.	Transverse E/A Profiles for Transtage Random Error Analysis	23
4.	Temperature Retrieval Error	24
5.	CO ₂ Concentration Retrieval Error	25

1. INTRODUCTION

In a recent study,⁽¹⁾ a formalism and computer code (EMABIC) were developed to invert profiles of plume infrared radiance and absorptance obtained in transverse scans across the lateral extent of test engine plumes near the nozzle exit plane in order to retrieve the radial profiles of temperature and gas species concentration in the plume flow field. Principal aspects of the formulation include: (1) the use of state-of-the-art band radiation models that treat highly nonuniform plumes and account for Doppler broadening effects; (2) the development of an iterative Abel inversion algorithm that allows the application of the well-known Abel inversion to nonthin optical sources; and (3) the formulation of a data smoothing procedure.

Consideration of smoothing is necessary to a successful inversion algorithm. Regardless of the inversion method used, experimental random noise on the input emission/absorption (E/A) profiles is amplified in the inversion process and can produce radial profiles so noisy that they are useless. The smoothing procedure used in EMABIC is a straightforward presmoothing of the input transverse E/A data before inversion.

The occurrence of random experimental error on the input profiles implies an associated error on the retrieved radial profiles. In the previous work, the propagation of errors through the inversion process was studied empirically by superimposing random errors on smooth transverse profiles and analyzing their effect on the retrieved radial profiles. In the present work, the formal theory of linear error propagation by transformation of the variance-covariance

-
1. S. J. Young, Inversion of Plume Radiance and Absorptance Data for Temperature and Concentration, AFRPL-TR-78-60, Air Force Rocket Propulsion Laboratory, Edwards Air Force Base, Calif. 29 September 1978.

error matrix of the data is applied. The resultant error propagation algorithm has been coded into EMABIC so that automatic error analysis can be made along with inversion.

The general theory of linear error propagation is well established,⁽²⁾ and only an outline and final results are presented here. This outline and application of the results to the present problem are treated in Section 2. A similar treatment of this problem has been made by Limbaugh.^(3,4) An example application of the method and comparison of results with the previous empirical results are made in Section 3. Preparation of control cards to operate EMABIC in the error propagation mode is described in an appendix.

-
2. A. A. Clifford, Multivariate Error Analysis, Applied Science Publishers Ltd., London, 1973.
 3. C. C. Limbaugh, An Uncertainty Propagation Analysis for an Infrared Band Model Technique for Combustion Gas Diagnostics, AEDC-TR-76-155, Arnold Engineering Development Center, Arnold Air Force Station, Tenn., April 1977.
 4. R. T. Shelby and C. C. Limbaugh, Smoothing Technique and Variance Propagation for Abel Inversion of Scattered Data, AEDC-TR-76-163, Arnold Engineering Development Center, Arnold Air Force Station, Tenn., April 1977.

2. ERROR PROPAGATION THEORY

2.1 General Theory

Consider a set of n equations defining n parameters y_i in terms of n observables x_i

$$y_i = y_i(x_1, x_2, \dots, x_n) \quad i = 1, n \quad (1)$$

The x_i represent measurable (observable) quantities, and we assume that we have a complete description of the measurements in the form of a set of mean values \bar{x}_i ($i = 1, n$), standard deviations $\sigma(x_i)$ ($i = 1, n$) and correlation coefficients $\rho(x_i, x_j)$ ($i, j = 1, n$). This last quantity is a measure of the degree of dependence between \bar{x}_i and \bar{x}_j . For $i = j$, $\rho(x_i, x_i) \equiv 1$.

The mean values of the parameters are calculated from Eq. (1) with the \bar{x}_i used in place of the x_i . Thus,

$$\bar{y}_i = y_i(\bar{x}_1, \bar{x}_2, \dots, \bar{x}_n) \quad i = 1, n \quad (2)$$

The functional dependence of the y_i on the x_i can be quite general for computing the mean values \bar{y}_i . In order to treat error propagation, however, we invoke a linearity approximation and write Eq. (1) to first order as

$$\delta y_i = \sum_{j=1}^n \frac{\partial y_i}{\partial x_j} \delta x_j \quad i = 1, n \quad (3)$$

where the partial derivatives are evaluated at the \bar{x}_i , $\delta y_i = y_i - \bar{y}_i$ and $\delta x_j = x_j - \bar{x}_j$. For this approximation to be reasonable, either the δx_j must be small or the equations must be nearly linear (so that second derivatives are small). Now define the partial derivative matrix \bar{A}

$$\bar{A} = \begin{bmatrix} \frac{\partial y_1}{\partial x_1} & \frac{\partial y_1}{\partial x_2} & \dots & \frac{\partial y_1}{\partial x_n} \\ \frac{\partial y_2}{\partial x_1} & \frac{\partial y_2}{\partial x_2} & & \vdots \\ \vdots & & & \vdots \\ \frac{\partial y_n}{\partial x_1} & \dots & & \frac{\partial y_n}{\partial x_n} \end{bmatrix} \quad (4)$$

and the error matrix of the observables

$$\bar{M}_X = \begin{bmatrix} \sigma^2(x_1) & \sigma(x_1) \sigma(x_2) \rho(x_1, x_2) \dots \sigma(x_1) \sigma(x_n) \rho(x_1, x_n) \\ \sigma(x_2) \sigma(x_1) \rho(x_2, x_1) & \sigma^2(x_2) & & \\ \vdots & & & \vdots \\ \sigma(x_n) \sigma(x_1) \rho(x_n, x_1) & \dots & & \sigma^2(x_n) \end{bmatrix} \quad (5)$$

This matrix is the variance-covariance matrix for the observable array x_i [$\sigma^2(x_i)$ is the variance of \bar{x}_i and $\sigma(x_i) \sigma(x_j) \rho(x_i, x_j)$ is the covariance between \bar{x}_i and \bar{x}_j]. The matrix is symmetric since $\rho(x_i, x_j) = \rho(x_j, x_i)$.

The corresponding variance-covariance matrix for the parameter array \bar{y}_i is

$$\bar{M}_Y = \bar{A} \bar{M}_X \bar{A}^T \quad (6)$$

where \bar{A}^T is the transpose of \bar{A} . Explicitly, the ij element of \bar{M}_y is

$$(\bar{M}_y)_{ij} = \sum_{k=1}^n \sigma(x_k) \frac{\partial y_i}{\partial x_k} \sum_{\ell=1}^n \sigma(x_\ell) \frac{\partial y_j}{\partial x_\ell} \rho(x_k, x_\ell) \quad (7)$$

with $\rho(x_k, x_k) \equiv 1$. The matrix \bar{M}_y has exactly the same structure as \bar{M}_x . The standard deviation of \bar{y}_i is

$$\sigma(y_i) = \sqrt{(\bar{M}_y)_{ii}} \quad (8)$$

and the correlation coefficient connecting \bar{y}_i and \bar{y}_j is

$$\rho(y_i, y_j) = \frac{(\bar{M}_y)_{ij}}{\sigma(y_i) \sigma(y_j)} \quad (9)$$

In the following sections, this general result will be applied to the propagation of errors through the data presmoothing operation and then through the profile inversion operation used in EMABIC. In the first application, the variance-covariance matrix \bar{M}_x is that of the raw, unsmoothed E/A data, and \bar{M}_y is the corresponding matrix for the smoothed E/A data. In the second application, \bar{M}_y of the smoothed data becomes the input matrix \bar{M}_x , and the computed \bar{M}_y describes the error characteristics of the recovered temperature and concentration profiles of the plume.

The elements of \bar{K} are

$$k_1 = (a_2^2 + b_1^2) \gamma + d_1$$

$$k_2 = -(a_2 b_2 + 2 b_1 c_1) \gamma$$

$$k_3 = a_2 c_2 \gamma$$

$$k_4 = k_2$$

$$k_5 = (a_3^2 + b_2^2 + 4 c_1^2) \gamma + d_2$$

$$k_6 = -(a_3 b_3 + b_2 c_2) \gamma$$

$$k_7 = a_3 c_3 \gamma$$

$$k_{5i-7} = k_{5i-13}$$

$$k_{5i-6} = k_{5i-9}$$

$$k_{5i-5} = (a_{i+1}^2 + b_i^2 + c_{i-1}^2) \gamma + d_i \quad \left. \begin{array}{l} \\ \\ \\ \\ \end{array} \right\} i = 3, M-2$$

$$k_{5i-4} = -(a_{i+1} b_{i+1} + b_i c_i) \gamma$$

$$k_{5i-3} = a_{i+1} c_{i+1} \gamma$$

$$k_{5M-13} = k_{5M-18}$$

$$k_{5M-12} = k_{5M-14}$$

$$k_{5M-11} = (b_{M-1}^2 + c_{M-2}^2) \gamma + d_{M-1}$$

(12)

where

$$\left. \begin{aligned} a_i &= \frac{1}{(z_{i+1} - z_{i-1})(z_i - z_{i-1})} \\ b_i &= \frac{1}{(z_{i+1} - z_i)(z_i - z_{i-1})} \\ c_i &= \frac{1}{(z_{i+1} - z_{i-1})(z_{i+1} - z_i)} \end{aligned} \right\} i = 1, M-1$$

(with $z_0 = -z_2$), $d_1 = z_2 - z_1$, $d_i = (z_{i+1} - z_{i-1})$ ($i = 2, M-1$), and γ is a smoothing parameter. (The pass through the loop with $i = 3$ in Eq. (12) will incorrectly define $k_8 = k_2$. This must be corrected to $k_8 = k_3$ after completing the loop. Also, the last pass through the loop will define k_{5M-13} incorrectly, but this is corrected automatically by the next definition after the loop.) Note that the order of the system has been reduced from M to $M-1$ because f_M is constrained to $f_M \equiv 0$.

The smoothing procedure is derived and discussed in Ref. 1. Briefly, the method consists of finding the function $f(z)$ that has the smoothest overall curvature but which does not differ from the unsmoothed function $g(z)$ by more than the estimated error of $g(z)$. As the smoothing parameter varies from $\gamma = 0$ to ∞ , the degree of smoothing varies from none to infinite. γ is selected as that value that satisfies

$$\frac{1}{R} \int_0^R [f(z, \gamma) - g(z)]^2 dr = \epsilon^2$$

where ϵ is a measure of the errors in $g(z)$. Smoothing is applied separately to \bar{N}_i and $1 - \bar{\tau}_i$ so that there are, in general, two smoothing parameters, $\gamma_{\bar{N}}$ and $\gamma_{\bar{\tau}}$.

Equation (10) is linear, and the partial derivative matrix, Eq. (4), to be used in Eqs. (6) or (7) to propagate errors to the smoothed profiles is just the matrix $\bar{H} = \bar{K}^{-1}$. The inversion required to get \bar{H} is performed in EMABIC with a standard⁽⁵⁾ Gaussian elimination routine designed for banded matrices. The variance-covariance matrix for the unsmoothed profile \bar{g}_i' is taken as the diagonal matrix

$$\bar{M}_{g'} = \begin{bmatrix} d_1^2 \sigma^2(g_1) & & & \\ & d_2^2 \sigma^2(g_2) & & \\ & & \ddots & \\ & & & d_{M-1}^2 \sigma^2(g_{M-1}) \end{bmatrix} \quad (13)$$

The lack of nonzero elements off the main diagonal results from the assumption that the transverse data have been collected with a spatial resolution Δz that is less than or equal to the data step size across $0 \leq z \leq R$. That is, $\Delta z \leq \min(z_i - z_{i-1})$. Then, there can be no correlation between measured values of \bar{g}_i and \bar{g}_j .

The resultant variance-covariance matrices for the smoothed E/A profiles are

$$\begin{aligned} \bar{M}_{N_s} &= \overline{\bar{H}(\gamma_N) M_{N'} H(\gamma_N)^T} \\ \bar{M}_{T_s} &= \overline{H(\gamma_T) M_{T'} H(\gamma_T)^T} \end{aligned} \quad (14)$$

5. System 1360 Scientific Subroutine Package (360A-CM-O3X) Version III, Programmers Manual, H20-0205-3, IBM Technical Publication Department, White Plains, N. Y., 1968.

or, explicitly,

$$\begin{aligned}
 (\bar{M}_{\bar{N}_s})_{ij} &= \sum_{k=1}^{M-1} h_{ik}(\gamma_{\bar{N}}) \sigma^2(\bar{N}_k) h_{jk}(\gamma_{\bar{N}}) d_k^2 \\
 (\bar{M}_{\bar{\tau}_s})_{ij} &= \sum_{k=1}^{M-1} k_{ik}(\gamma_{\bar{\tau}}) \sigma^2(\bar{\tau}_k) h_{jk}(\gamma_{\bar{\tau}}) d_k^2
 \end{aligned}
 \tag{15}$$

where $h_{ij}(\gamma_{\bar{N}})$ and $h_{ij}(\gamma_{\bar{\tau}})$ are elements of $\bar{H}(\gamma_{\bar{N}})$ and $\bar{H}(\gamma_{\bar{\tau}})$, respectively. Note that, although the variance-covariance matrices of the unsmoothed profiles are diagonal, the matrices for the smoothed profiles need not be. With increasing γ , the correlation between elements \bar{f}_i and \bar{f}_j can become quite large.

In order to handle data from some experimental programs, ⁽¹⁾ EMABIC allows values of M up to 301. Thus \bar{H} could be as large as 300×300 . Both $\bar{M}_{\bar{N}_s}$ and $\bar{M}_{\bar{\tau}_s}$ could presumably then also be each 300×300 . The need to retain three matrices of this size strains the storage capacity of many computers. Accordingly, the order of $\bar{M}_{\bar{N}_s}$ and $\bar{M}_{\bar{\tau}_s}$ is reduced in size to $N \times N$ where N is the number of radial/transverse zones used in inversion and has a maximum value of 50. The reduction in size is accomplished by simple linear interpolation on the four elements $(\bar{M}_{f_s})_{i,j}$, $(\bar{M}_{f_s})_{i,j+1}$, $(\bar{M}_{f_s})_{i+1,j}$ and $(\bar{M}_{f_s})_{i+1,j+1}$ that immediately surround the grid points $z_n = (n-1)\Delta + \Delta/2$, $z_m = (m-1)\Delta + \Delta/2$ where $n, m = 1, N$ and $\Delta = R/N$. The reduced matrices $\bar{M}_{\bar{N}_s}$ and $\bar{M}_{\bar{\tau}_s}$ then represent the variance-covariance matrices for the smoothed profiles at the centers of the N transverse zones and are the input error matrices for the subsequent error propagation through the inversion step.

2.3 Error Propagation through Inversion

The inversion process of EMABIC is an iterative solution of the equations of radiative transfer defining $\bar{N}(z)$ and $\bar{\tau}(z)$ as integrals over functions of $T(r)$ and $c(r)$. The numerical quadrature approximations to these equations define \bar{N}_i and $\bar{\tau}_i$ ($i=1, N$) in terms of T_j and c_j ($j=1, N$) by

$$\left. \begin{aligned} \bar{N}_i &= \bar{N}_i(T_i, T_{i+1}, \dots, T_N, c_i, c_{i+1}, \dots, c_N) \\ \bar{\tau}_i &= \bar{\tau}_i(T_i, T_{i+1}, \dots, T_N, c_i, c_{i+1}, \dots, c_N) \end{aligned} \right\} i = 1, N \quad (16)$$

The inversion process solves this set of nonlinear equations to give

$$\left. \begin{aligned} T_j &= T_j(\bar{N}_j, \bar{N}_{j+1}, \dots, \bar{N}_N, \bar{\tau}_j, \bar{\tau}_{j+1}, \dots, \bar{\tau}_N) \\ c_j &= c_j(\bar{N}_j, \bar{N}_{j+1}, \dots, \bar{N}_N, \bar{\tau}_j, \bar{\tau}_{j+1}, \dots, \bar{\tau}_N) \end{aligned} \right\} j = 1, N \quad (17)$$

From Eq. (3), the equations describing linear error propagation are

$$\left. \begin{aligned} \delta T_j &= \sum_{i=j}^N \frac{\partial T_j}{\partial \bar{N}_i} \delta \bar{N}_i + \sum_{i=j}^N \frac{\partial T_j}{\partial \bar{\tau}_i} \delta \bar{\tau}_i \\ \delta c_j &= \sum_{i=j}^N \frac{\partial c_j}{\partial \bar{N}_i} \delta \bar{N}_i + \sum_{i=j}^N \frac{\partial c_j}{\partial \bar{\tau}_i} \delta \bar{\tau}_i \end{aligned} \right\} j = 1, N \quad (18)$$

(Note that these equations are triangular because the value of a transverse variable at z does not depend on the form of any radial function for $r < z$.) The appropriate partial derivative matrix for error propagation is then

$$\bar{A} = \left[\begin{array}{ccc|ccc} \frac{\partial T_1}{\partial \bar{N}_1} & \frac{\partial T_1}{\partial \bar{N}_2} & \dots & \frac{\partial T_1}{\partial \bar{N}_N} & \frac{\partial T_1}{\partial \bar{\tau}_1} & \frac{\partial T_1}{\partial \bar{\tau}_2} & \dots & \frac{\partial T_1}{\partial \bar{\tau}_N} \\ & \frac{\partial T_2}{\partial \bar{N}_2} & & \vdots & & \frac{\partial T_2}{\partial \bar{\tau}_2} & & \vdots \\ & & \dots & \frac{\partial T_N}{\partial \bar{N}_N} & & & \dots & \frac{\partial T_N}{\partial \bar{\tau}_N} \\ \hline \frac{\partial c_1}{\partial \bar{N}_1} & \frac{\partial c_1}{\partial \bar{N}_2} & \dots & \frac{\partial c_1}{\partial \bar{N}_N} & \frac{\partial c_1}{\partial \bar{\tau}_1} & \frac{\partial c_1}{\partial \bar{\tau}_2} & \dots & \frac{\partial c_1}{\partial \bar{\tau}_N} \\ & \frac{\partial c_2}{\partial \bar{N}_2} & & \vdots & & \frac{\partial c_2}{\partial \bar{\tau}_2} & & \vdots \\ & & \dots & \frac{\partial c_N}{\partial \bar{N}_N} & & & \dots & \frac{\partial c_N}{\partial \bar{\tau}_N} \end{array} \right] \quad (19)$$

The inverse equations, Eq. (17), are not known explicitly and thus the partial derivatives of Eq. (19) cannot be calculated. The partial derivatives $\bar{N}/\partial T$, $\bar{N}/\partial c$, $\bar{\tau}/\partial T$ and $\bar{\tau}/\partial c$ can, however, be computed with the radiation calculation routines of EMABIC. The derivatives are computed numerically. For example, the array of derivatives $\partial \bar{N}_i / \partial T_j$ ($i = 1, N$) are, in principle, computed from

$$\frac{\partial \bar{N}_i}{\partial T_j} = \frac{N_i^+ - N_i^-}{2\epsilon} \quad (20)$$

where

$$\begin{aligned} \bar{N}_i^+ &= \bar{N}_i [T_i, T_{i+1}, \dots, (1+\epsilon) T_j, \dots, T_N, c_i, c_{i+1}, \dots, c_N] \\ \bar{N}_i^- &= \bar{N}_i [T_i, T_{i+1}, \dots, (1-\epsilon) T_j, \dots, T_N, c_i, c_{i+1}, \dots, c_N] \end{aligned} \quad (21)$$

The profiles \bar{N}_i^+ and \bar{N}_i^- ($i = 1, N$) are computed with the T_j and c_j obtained from the inversion. ϵ is a small parameter ($\epsilon = 0.01$ is generally used). The process is repeated for all j to get the full matrix of $\partial \bar{N}_i / \partial T_j$. The three remaining derivative arrays are computed in the same manner. In practice, the derivatives are computed in a slightly different manner. The derivatives considered so far refer to changes of transverse variables at transverse zone centers with respect to variations at radial zone centers, or, vice versa. The computation routines of EMABIC do not operate on variables defined at zone centers, but rather at zone boundaries. Thus, Eqs. (20) and (21) are used to compute the four partial derivatives corresponding to the corners of the intersection of the i th transverse and j th radial zone, and the derivative, Eq. (20) approximated as the average of these four values. The reason for operating on zone centers instead of zone boundaries is discussed below.

From the derivatives just discussed, the matrix

$$\bar{B} = \left[\begin{array}{ccc|ccc} \frac{\partial \bar{N}_1}{\partial T_1} & \frac{\partial \bar{N}_1}{\partial T_2} & \dots & \frac{\partial \bar{N}_1}{\partial T_N} & \frac{\partial \bar{N}_1}{\partial c_1} & \frac{\partial \bar{N}_1}{\partial c_2} & \dots & \frac{\partial \bar{N}_1}{\partial c_N} \\ & \frac{\partial \bar{N}_2}{\partial T_2} & & \vdots & & \frac{\partial \bar{N}_2}{\partial c_2} & & \vdots \\ & & \dots & \frac{\partial \bar{N}_N}{\partial T_N} & & & \dots & \frac{\partial \bar{N}_N}{\partial c_N} \\ \hline \frac{\partial \bar{\tau}_1}{\partial T_1} & \frac{\partial \bar{\tau}_1}{\partial T_2} & \dots & \frac{\partial \bar{\tau}_1}{\partial T_N} & \frac{\partial \bar{\tau}_1}{\partial c_1} & \frac{\partial \bar{\tau}_1}{\partial c_2} & \dots & \frac{\partial \bar{\tau}_1}{\partial c_N} \\ & \frac{\partial \bar{\tau}_2}{\partial T_2} & & \vdots & & \frac{\partial \bar{\tau}_2}{\partial c_2} & & \vdots \\ & & \dots & \frac{\partial \bar{\tau}_N}{\partial T_N} & & & \dots & \frac{\partial \bar{\tau}_N}{\partial c_N} \end{array} \right] \quad (22)$$

is constructed. Its inverse is the desired propagation matrix \bar{A} , that is,

$$\bar{A} = \bar{B}^{-1} \quad (23)$$

The inversion of \bar{B} is carried out with a standard Gaussian elimination algorithm using maximal pivot strategy.⁽⁶⁾

The objection to formulating the error propagation formalism on zone boundaries is that the resulting derivative matrix corresponding to (22) is singular and cannot be inverted. The singularity results because partial derivatives evaluated at $i=j=N+1$ are identically zero.

The variance-covariance matrices for propagation through the inversion matrix \bar{A} were treated in Section 2.2, but separately. In order to be consistent with \bar{A} , which accounts for the coupling of \bar{N} and $\bar{\tau}$, the appropriate error matrix is constructed from $\bar{M}_{\bar{N}_s}$ and $\bar{M}_{\bar{\tau}_s}$ as the $2N \times 2N$ matrix

$$\bar{M}_{\bar{N}\bar{\tau}} = \begin{bmatrix} \bar{M}_{\bar{N}_s} & | & \\ \hline & | & \bar{M}_{\bar{\tau}_s} \\ \hline & | & \end{bmatrix} \quad (24)$$

The assignment of zero to the off-diagonal quadrants of this matrix reflects the usual experimental condition that the radiance and absorptance data are measured independently from each other. Thus there is no correlation between \bar{N}_i and $\bar{\tau}_j$ even for $i=j$.

6. B. Carnahan, H. A. Luther and J. O. Wilkes, Applied Numerical Methods, John Wiley and Sons Inc., N. Y., 1969, p. 282.

Finally, the variance-covariance matrix for the recovered temperature and concentration profiles is

$$\bar{M}_{Tc} = \overline{A \bar{M}_{N\tau} A^T} \quad (25)$$

The first N elements on the diagonal of \bar{M}_{Tc} are the recovered temperature variances, and the last N elements are the concentration variances. Explicitly, these are

$$\begin{aligned} \sigma^2(T_j) &= \sum_{k=1}^N A_{jk} \sum_{l=1}^N (\bar{M}_{N\tau})_{kl} A_{jl} \\ &+ \sum_{k=1}^N A_{j, k+N} \sum_{l=1}^N (\bar{M}_{N\tau})_{kl} A_{j, l+N} \end{aligned} \quad (26)$$

$$\begin{aligned} \sigma^2(c_j) &= \sum_{k=1}^N A_{j+N, k} \sum_{l=1}^N (\bar{M}_{N\tau})_{kl} A_{j+N, l} \\ &+ \sum_{k=1}^N A_{j+N, k+N} \sum_{l=1}^N (\bar{M}_{N\tau})_{kl} A_{j+N, l+N} \end{aligned} \quad (27)$$

3. EXAMPLE APPLICATION

An empirical analysis was made in a previous study⁽¹⁾ of error propagation for temperature, H₂O concentration and CO₂ concentration retrieval from E/A data obtained on a Transtage engine. The present error propagation formalism is applied here to temperature and CO₂ concentration retrieval for the same conditions as the previous analysis. From a number of successful inversions of the Transtage data, the temperature and CO₂ concentration profiles of Fig. 1 were obtained. In the previous empirical analysis, these profiles, along with the pressure profile of Fig. 2 were used to generate the transverse E/A profiles of Fig. 3. Random errors were then superimposed on the E/A data at the M=201 equally spaced points between z=0 and z=R=67cm. The rms magnitude of the errors was 3% of peak value ($\sigma=0.0048 \text{ W/cm}^2\text{-sr-}\mu\text{m}$) for radiance and 5% of peak value ($\sigma=0.0093$) for absorptance. These profiles are shown in Fig. 3 and essentially model the original unsmoothed Transtage data. The noisy E/A profiles were then smoothed and inverted to retrieve the radial T c profiles. The process of error superposition, smoothing and inversion was carried out five times. For all five cases, smoothing parameter values of $\gamma_{\bar{N}} = 675$ and $\gamma_{\bar{\tau}} = 2700$ were used. The resultant five sets of retrieved T c profiles were then used to compute the standard deviations of T and c as a function of r. The results are shown in Figs. 4 and 5.

In the present analysis, no smoothing or inversion is necessary. We can proceed directly from the radial profiles of Figs. 1 and 2 (needed to compute the partial derivatives $\partial\bar{N}/\partial T$, $\partial\bar{N}/\partial c$, $\partial\bar{\tau}/\partial T$ and $\partial\bar{\tau}/\partial c$) and the data for M, R, $\sigma(\bar{N}_i)$, $\sigma(\bar{\tau}_i)$, $\gamma_{\bar{N}}$ and $\gamma_{\bar{\tau}}$ already given. The resultant standard deviations $\sigma(T_i)$ and $\sigma(c_i)$ $i=1, N$ for $N=5, 10$ and 20 are shown in Figs. 4 and 5.

The results are essentially in agreement with those obtained in the previous analysis. The present analysis yields σ values that are ~ 2 times larger than the empirical results. This difference may be due in part either to the limited sample (5) used to compute the empirical results or to the fact that the empirical

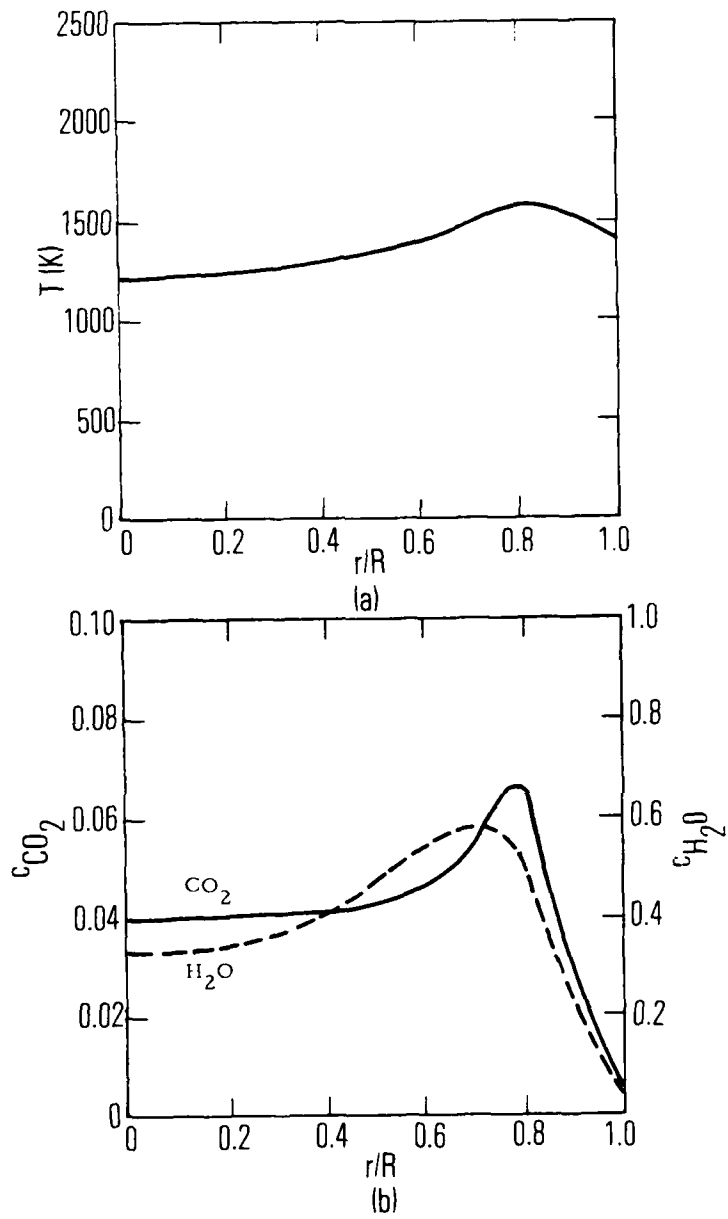


Fig. 1. Transtage Temperature and Gas Concentration Profiles.
 (a) Temperature; (b) Concentrations.

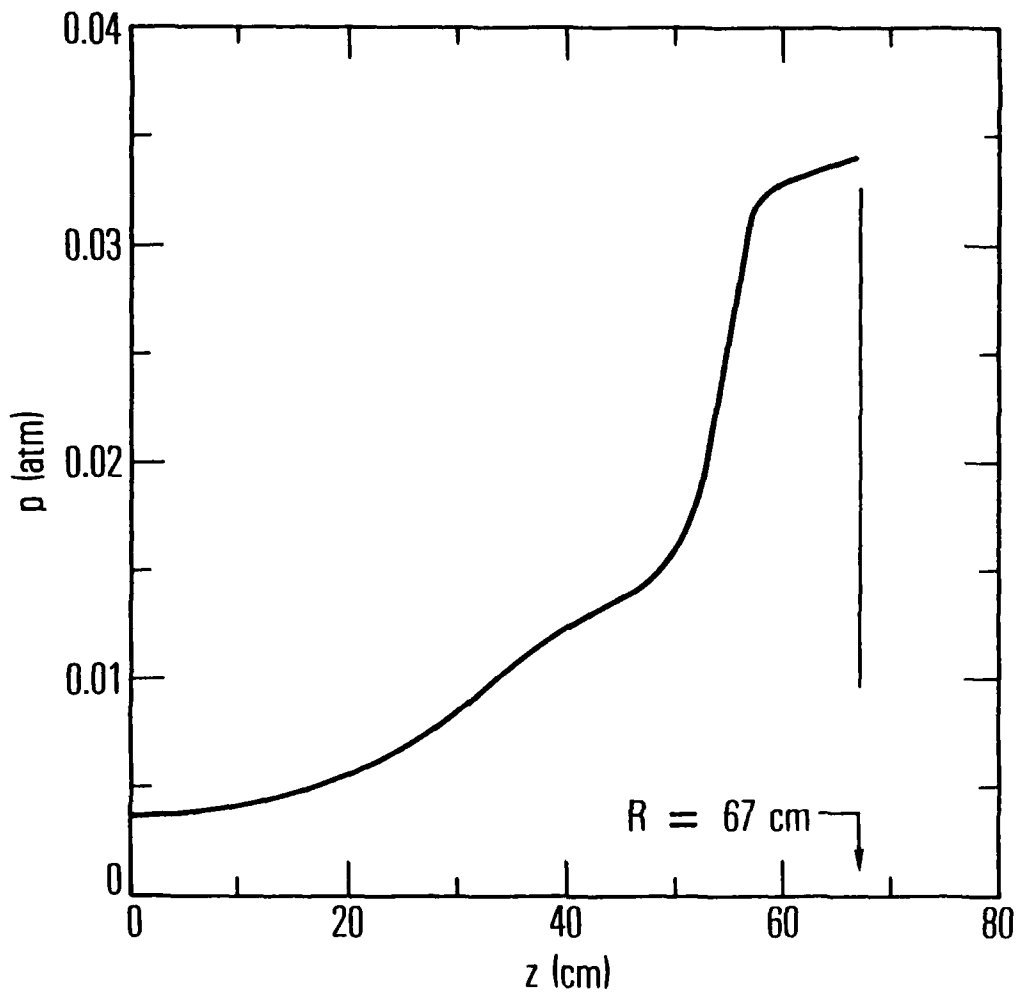


Fig. 2. Transtage Pressure Profile.

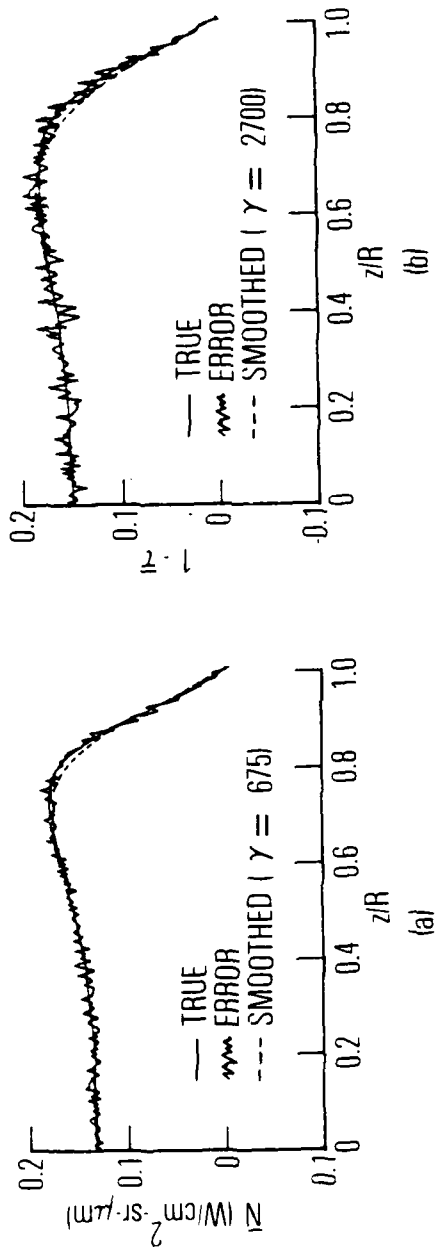


Fig. 3. Transverse E/A Profiles for Transtage Random Error Analysis. (a) Radiance; (b) Absorptance.

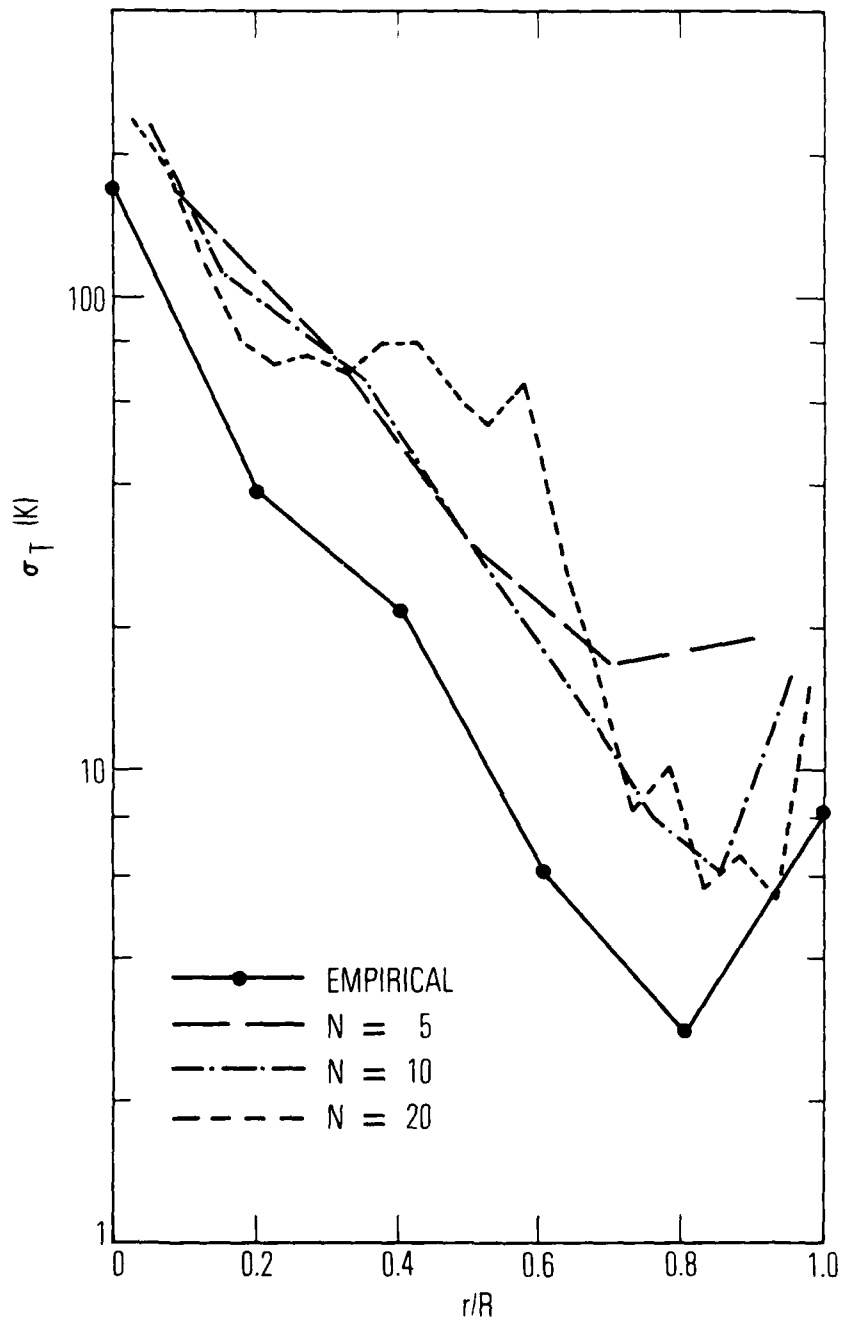


Fig. 4. Temperature Retrieval Error.

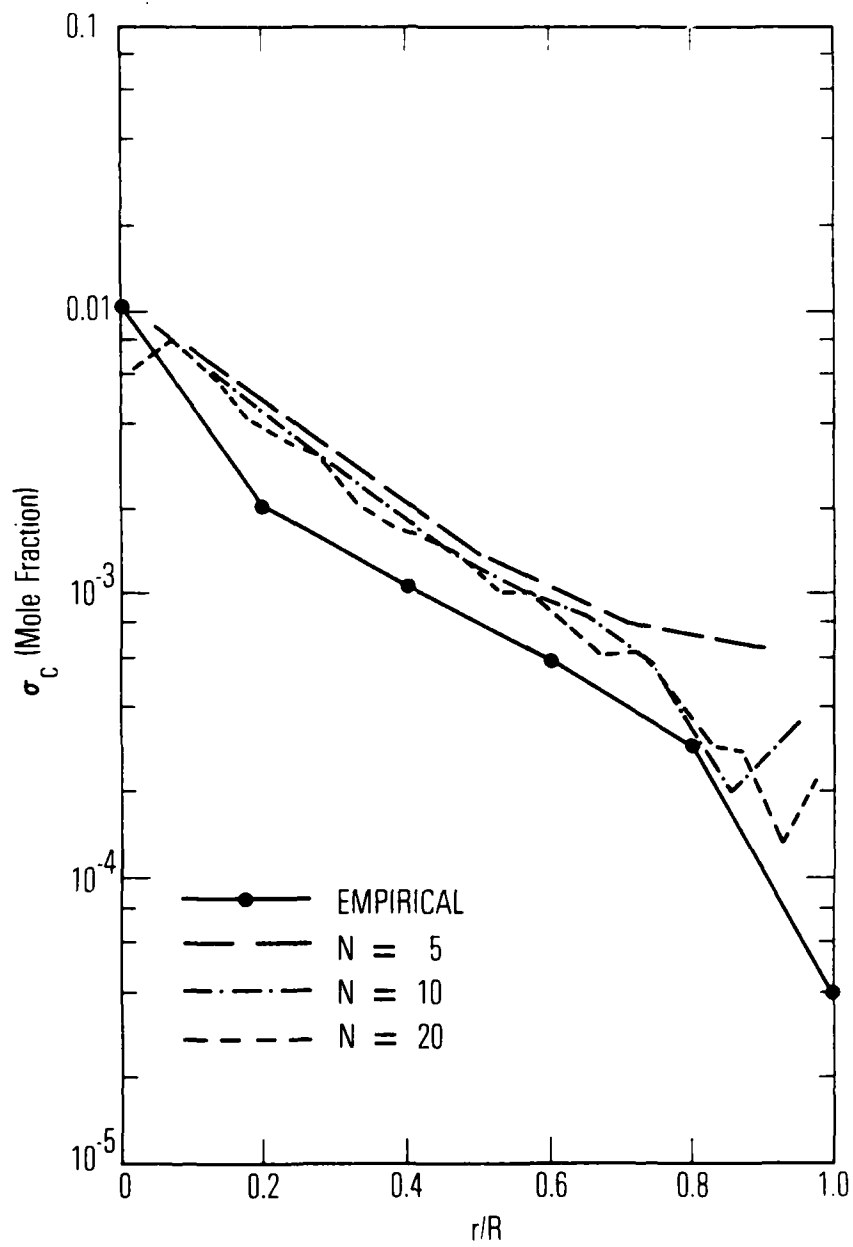


Fig. 5. CO_2 Concentration Retrieval Error.

procedure allows for nonlinear error propagation while the present analysis employs a linear approximation.

The variation of the results with N shows only an increasing structure with increasing N but no consistent trend to change the overall magnitude of the estimated errors.

APPENDIX

ERROR PROPAGATION CONTROL CARDS FOR EMABIC

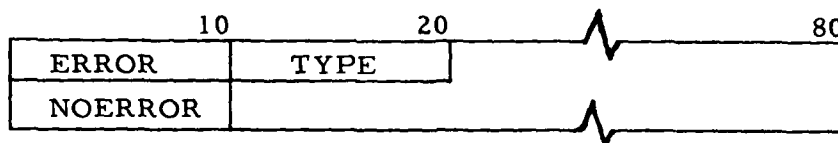
The incorporation of error propagation into EMABIC requires a slight modification and enlargement of the instructions for data preparation given in Chapter IV of Ref. 1.

The first change allows the input of experimental error data along with the transverse data itself. In Fig. 6 (p. 65) of Ref. 1, $\sigma_{\bar{N}}(i)$ and $\sigma_{\bar{\tau}}(i)$ should be entered in columns 31-40 and 41-50, respectively, on the same cards that enter $\bar{N}(i)$ and $\bar{\tau}(i)$. The legend of Fig. 6 should include the following:

$$\left. \begin{aligned} \sigma_{\bar{N}}(i) &= \text{estimated rms error of } \bar{N}(i) \\ \sigma_{\bar{\tau}}(i) &= \text{estimated rms error of } \bar{\tau}(i) \end{aligned} \right\} \begin{array}{l} \text{Units consistent with } \bar{N}(i) \\ \text{and } \bar{\tau}(i) \end{array}$$

The second change concerns the List Control Card. In the section on card type 10 (p. 64), the last sentence should read, "If the variable JKLIST (format A10) on the LIST card has the value PRINT, the emission and absorption functions $J(r)$ and $K(r)$ are also listed for each iteration."

The additions are two new control cards named ERROR and NOERROR. The following addition should be made to Fig. 3 (p. 58)



and the following section added after the discussion of the Execution Control Card (pp. 66-67).

13. Error Control Cards Two cards with the names ERROR and NOERROR control error propagation calculations. An ERROR card indicates that an error propagation analysis should be made in either the Abel or iterative Abel inversion mode. If TYPE (format IJ) has the integer value 0 or blank, the error analysis will be performed immediately following a successful inversion run in which E/A data have been inputed. An error analysis does not require an inversion. If TYPE has the value 1, an error analysis will be performed using the error data read in from the transverse data deck and the pTc data read in from a profile generation mode deck. A SPECIE card must be used in this mode.

The TYPE=1 mode allows an error analysis to be made for hypothetical experiments. For example, if first-order estimates of radial profiles are already known, and likely experimental errors are known from previous experience (or are estimated), it can be determined whether or not an experimental program is likely to improve on the first-order estimates of the radial profiles.

The NOERROR card turns off any error analysis for subsequent runs.